

DOI: 10.1002/ 201804856

Article type: Full Paper

Addition Effect of Pyreneammonium Iodide to Methylammonium Lead Halide Perovskite-2D/3D Hetero Structured Perovskite with Enhanced Stability

*Fu Yang**, *Putao Zhang*, *Muhammad Akmal Kamarudin*, *Gaurav Kapil*, *Tingli Ma*, *Shuzi Hayase**

F. Yang, P. T Zhang, Dr. M. A. Kamarudin, Dr. G. Kapil, Prof. Dr. T. L. Ma, Prof. Dr. S. Hayase

Graduate School of Life Science and Systems Engineering Institution Kyushu Institute of Technology

2-4 Hibikino Wakamatsu-ku, Kitakyushu 808-0196, Japan

E-mail: yang-fu@edu.life.kyutech.ac.jp; hayase@life.kyutech.ac.jp

Keywords: Two-dimensional; MAPbI₃; Planar solar cells; Stability; UV light stability.

Abstract

Despite the eminent performance of the organometallic halide perovskite solar cells (PSCs), the poor stability for humidity and ultraviolet irradiation is still major problem for the commercialization of PSCs. Herein, a novel functional organic compound 1-(ammonium acetyl)pyrene (PEYI) has successfully introduced for preparing the 2D/3D Hetero structured MAPbI₃ perovskite. Because of the functional organic pyrene group with high humidity resistance and strong absorption in the ultraviolet region, the 2D/3D perovskite film showed notable stability with no degradation in ~60% relative humidity after even 6 months and exhibited a high ultraviolet irradiation stability which kept nearly no degradation after one hour in the UV Ozone treatment. Planar PSCs were fabricated in the ~60% relative humidity air outside glovebox. The champion efficiency of (PEY₂PbI₄)_{0.02}MAPbI₃ perovskite solar cells was 14.7 % with nearly no hysteresis which is equal performance of 3D MAPbI₃ devices (15.0%). This work presents a new direction for enhancing the solar cells` performance and stability by incorporating a functional organic aromatic compound into the perovskite layer.

Introduction

Three-dimensional (3D) perovskite-based solar cells (PSCs) employing halide perovskite with organic cations have now showed power conversion efficiency of more than 22% at an unprecedented rate.^[1] However, there are still some challenge problems limiting the commercialization and mass production, such as instability and J-V hysteresis.^[2] Methyl ammonium lead iodide (MAPbI₃) and other perovskite materials still showed poor performances against humidity, heat and light soaking.^[3] Moreover, other additional degradation by UV irradiation, molecular oxygen also restrict the performances.^[4] Therefore, research in the area for designing more stable PSCs is highly necessary. Recently, it has been reported that two-dimensional (2D) PSCs exhibited the high stability. These 2D perovskites are described as (RNH₃)₂(MA)_{n-1}Pb_nI_{3n+1} (where RNH₃ usually is PEA= C₆H₅(CH₂)₂NH³⁺, BA=n-butylammonium) as absorbers in PSCs.^[5] Despite the high stability, the efficiency of 2D PSCs is still lower than 3D PSCs. To solve this problem, 2D/3D stacking structures, which have both advantage of 2D and 3D perovskite materials were reported.^[6] Stabilities of PSCs was enhanced with notable efficiency by introducing a thin 2D perovskite layer because these 2D perovskites would wrap the grain boundary and surface of 3D perovskites. However, most exploited 2D/3D perovskites are based on PEAI and BA organic compound, which prevent the research progress of the 2D/3D perovskites. In addition, there are many organic compound with functional group which could be useful for introducing into the perovskite layer to make the perovskite layer functional. Therefore, it is challenging and meaningful for researchers to find novel functional organic materials for the 2D/3D perovskite materials.

Herein, we introduced a new organic compound, 1-(ammonium acetyl)pyrene (PEY) as the 2D cation for preparing a new 2D/3D hetero structure. The 2D/3D perovskite has the advantage

of both the longtime stability of 2D perovskite and excellent carrier's transport of the 3D perovskite, showed nearly no degradation after more than 6 months kept in ~60% RH air atmosphere. While the normal 3D MAPbI₃ perovskite layer quickly degraded within two weeks. Moreover, the (PEY₂PbI₄)_{0.02}MAPbI₃ 2D/3D perovskite film showed nearly no degradation upon 60 minutes UV-Ozone treatment, which indicated the high resistance of the UV light and molecular oxygen. Furthermore, the best planar solar cell of (PEY₂PbI₄)_{0.02}MAPbI₃ 2D/3D perovskite devices showed a high efficiency of 14.7 % with nearly no hysteresis, and ultra-stable PSCs with no efficiency loss than 3D PSCs after kept in ~60% RH air atmosphere for more than 400 hours.

Results and Discussion

In this report, the composition of (PEY₂PbI₄)_xMAPbI₃ (x: 0, 0.02, 0.05, and 0.10) is abbreviated as 2D/3D-X, i. e. (PEY₂PbI₄)_{0.02}MAPbI₃ is abbreviated as 2D/3D-0.02. Figure 1 shows the X-ray diffraction (XRD) patterns 2D/3D-X (x: 0, 0.02, 0.05, and 0.10) perovskite films with different PEY content on glass substrates. All the films were prepared in an around 60% RH open air condition. In all 2D/3D-X, strong diffraction peaks located on 14.1°, 28.4° and 31.9° for the 2θ scan were observed and they correspond to the planes of (110), (220) and (222), which is in coincident to the previous reports.^[7] The result conformed that all the films of 2D/3D-X contain highly crystalized perovskite phase.^[8] Furthermore, a weak diffraction pattern of PbI₂ appeared at around 12.7° in 2D/3D-0 films and the intensity of the peak decreased with an increase in x from 0 to 0.1. The 2D peaks appeared at 6.6° and 9.2° were observed in 2D/3D-0.10. These peak intensities decreased as x decreases from 0.1 to 0 (Figure S2). It was noted that the increased concentration of PEY resulted in the completed PbI₂ transformation. This maybe owing to the enhanced humidity resistance of 2D layer, which prevent MAI and PbI₂ from the moisture in the spin-coating progress.

The stability the 2D/3D-X films were tested by tracing the variation of the XRD patterns. Change of XRD patterns after storage in air atmosphere is also summarized in Figure 1. As shown in Figure 1a, for 2D/3D-0, peak at (110) of MAPbI₃ became very weak after the sample was stored in two weeks. In addition, several peaks appeared, one of which is 12.7 ° assigned as PbI₂. This indicates the 3D MAPbI₃ perovskite started to decompose immediately after exposed to open air because of loss of MA. In contrast, as shown in Figure 1b, c, d, for 2D/3D-0.02, 2D/3D-0.05, 2D/3D-0.10, peak at (110) of 3D MAPbI₃ did not change after more than 6 months, leading to the conclusion that only 0.02 addition of PEY can greatly enhance the stability of these perovskite layers. The UV-vis spectra of the 2D/3D-X perovskite film tested by different time also clearly exhibits the enhanced stability of the perovskite layer by PEY incorporation. As shown in Figure S4, the UV absorption decreased totally for MAPbI₃ perovskite film within two weeks. However, for keeping at about 60% RH atmosphere for more than 6 months, almost no difference of the absorption intensity can be detected for the 2D/3D-x (x= 0.02, 0.05, 0.1) perovskite films, which showed the excellent moisture stability of the materials. The insert optic figures of the perovskite films show 2D/3D-x (x= 0.02, 0.05, 0.1) perovskite films kept as a shining film after even more than 6 months.

Figure 2a showed the light absorption spectra for 2D/3D-X (x, 0, 0.02, 0.05, 0.10) perovskite films on FTO glass substrates. It was found that the absorbance intensity decreased and the absorption edge blue-shifted as x increased from 0 to 0.10. Meanwhile, E_g shifted from 752 nm (1.57 eV) for 2D/3D-0 to 735 nm (1.60 eV) for 2D/3D-0.10 as shown in Figure 2b. These results shows that 2D structure is created in the 3D structure. The valence band edge was shifted from -5.58 eV for 2D/3D-0 to more negative values of -5.60 eV, -5.63 eV, and -5.68 eV for 2D/3D-0.02, 2D/3D-0.05, and 2D/3D-0.10, respectively, as determined by photoelectron spectroscopy (Figure 2c). The observation is in agreement of conventional consideration that predict destabilization of valence band.^[9] Figure 2d summarizes shift of conduction band and

valence band which were obtained from the valence band energy level and optical absorption edge. It is clear shown in Figure 2d that the electronic configuration of MAPbI₃ suffers only minor changes when 2D structure was introduced low content 2D, which is critical in terms of keeping high photovoltaic performance of the MAPbI₃ 3D perovskite materials.

Next, the contact angle tests were used to test the water resist ability of 2D/3D-X films. The water contact angle of 2D/3D-0 film was 29.6°. This contact angle was increased to 105°, 107.9°, and 112.7° for 2D/3D-0.02, 2D/3D-0.05, 2D/3D-0.10, respectively, as shown in Figure S6. When water was dripped on 2D/3D-X films, color for 2D/3D-0 film changed immediately from dark to yellow, however, 2D/3D-0.02 survived during 30 seconds (Figure S7). These results would be explained by the water repelling behavior of PEY, which was introduced in the 3D perovskite. The high moisture resistance could be owing to the high hydrophobicity of the pyrene group.

As perovskite can be easy degraded by UV irradiation and molecular oxygen. Therefore, UV Ozone machine was utilized to test the stability of the 2D/3D-X perovskite film which shown in Figure 3. The UV-vis absorbance gradually decreased when 2D/3D-0 film was exposed to UV Ozone treatment as shown in Figure 3a. However, there was nearly no change of the UV-vis absorbance for 2D/3D-0.02 after the films was exposed to UV Ozone for more than 60 minutes as shown in Figure 3b. From the color of the perovskite film we can clear see that after 60 minutes, the 2D/3D-0 perovskite film change from dark to yellow slightly. While for the 2D/3D-0.02 perovskite, the film color showed nearly no change. The corresponding XRD of color changed perovskite films after UV Ozone treatment are shown in Figure S5. These results show the enhanced stability against light irradiation and oxidations for the film consisting of PEY.

Figure 4 showed the surface morphology of 2D/3D-X ($x= 0, 0.02, 0.05, 0.10$) film on FTO/compact SnO₂ substrate. All the films showed a dense pinhole free morphology. However, there was a lot PbI₂ residue on surface of MAPbI₃ perovskite film, which was shown the white spot in Figure 4a.^[10] Thelakkat and coworkers proved that the rate of degradation of CH₃NH₃PbI₃ could be accelerated because of PbI₂ residue present in the perovskite film.^[11] Moreover, researchers have proved that the surface defects and trap state density originate from the uncoordinated Pb atoms of the residue PbI₂ which would limit the performances of PSCs.^[12] As shown in Figure 4b, c and d, these residues were not observed in 2D/3D-X ($x=0.02, 0.05, 0.10$). These results were in consistent of the XRD date shown in Figure 1. The grain size was decreased gradually with the increase in X value of 2D/3D-X, as shown in Figure 4e-h. The statistical grain size for the perovskite films is shown in Figure S8.^[13]

To investigate the effect of 2D/3D perovskite on the photo voltaic performance, the planar PSCs using SnO₂ as the electron transport layer and 2,2',7,7'-tetrakis (N,N-di-p-methoxyphenylamino)-9,9-spirobifluorene (spiro-OMeTAD) as the hole transport layer as shown in Figure 5a. These results are summarized in Figure 5b, c and d. The champion PCE of 2D/3D-0 devices was 15.0 % with J_{sc} of 21.85 mA/cm², V_{oc} of 1.01V and FF of 68.2 %. The performance of 2D/3D-0.02 showed equal compared with the 2D/3D-0 perovskite with a champion PCE of 14.7 %, with J_{sc} of 21.15 mA/cm², V_{oc} of 1.05 V and FF of 66.1 %. The J_{sc} and FF of the 2D/3D-0.02 devices were slightly lower than 2D/3D-0 devices which may be owing to the reduced charge mobility of the 2D perovskite.^[14] The V_{oc} of 2D/3D-0.02 was higher than that of 2D/3D-0 maybe owing to the increased bandgap.

Hysteresis index (HI) values were calculated from the J-V curves.^[15] A modified hysteresis index (HI) values is defined by equation 1. The HI value of 2D/3D-0.02 was 0.02, which was less than 2D/3D-0 (HI, 0.21). This result shows introduction of PEY was able to eliminate effectively hysteresis behaviors. Figure 5b and 5e show the J-V curves and the corresponding

IPCE curves of the champion devices. The IPCE curve for 2D/3D-0.02 has higher value at short wavelength and lower at longer wavelength, compared with that for 2D/3D-0.02. This may be explained by the little lower absorption for 2D/3D-0.02 at 700-800 nm region, as shown in Figure 2a. The IPCE edge was about 800 nm, which is consistent to that of light absorption. Indoor environment stability for 2D/3D-0.02 and 2D/3D-0 were investigated as shown in Figure 5f. The unsealed devices were stored in ~60% RH and dark air atmosphere. 2D/3D-0 device degraded to 51.6% of its initial efficiency after 400 hours. However, for 2D/3D-0.02 device, the PCE was still kept with no decline after 400 hours. From all the results, it was proved that 2D/3D-0.02 perovskite devices has enhanced stability with keeping the high efficiency of 2D/3D-0.

Conclusion

In conclusion, we have successfully introduced pyreneammonium iodide as the 2D layer for preparing the 2D/3D perovskite. The 2D/3D perovskite solar cell showed notable stability, which there is no degradation in ~60% RH humidity after 6 months. Moreover, the 2D/3D perovskite also showed a high UV stability which kept nearly no degradation after one hour in the UV Ozone treatment. The contact angel can reached beyond 100° that is more 3.5 times than 2D/3D-0 perovskite layer (29.6°). The champion efficiency of 2D/3D-0.02 perovskite solar cells is 14.7% which is almost equal to the performance of 2D/3D-0 devices (15.0%) with nearly no hysteresis. This work provides a novel concept for incorporating the functional organic compounds into the perovskite layer to enhance the solar cells` performance.

Supporting Information

Experimental details. Optic images, UV-vis spectra and XRD diffraction of 2D/3D perovskite film. Contact-angle test of 2D/3D-0 and 2D/3D-0.02 perovskite film. Photovoltaic statistics of the perovskite solar cells. Detail information of the XRD peak.

Acknowledgements

This research was supported by Core Research for Evolutional Science and Technology (CREST) project of Japan Science and Technology

Received: ((will be filled in by the editorial staff))

Revised: ((will be filled in by the editorial staff))

Published online: ((will be filled in by the editorial staff))

References

- [1] a) M. M. Lee, J. Teuscher, T. Miyasaka, T. N. Murakami, H. J. Snaith, *Science* **2012**, 338, 643; b) H. Zhou, Q. Chen, G. Li, S. Luo, T.-b. Song, H.-S. Duan, Z. Hong, J. You, Y. Liu, Y. Yang, *Science* **2014**, 345, 542; c) K. Domanski, E. A. Alharbi, A. Hagfeldt, M. Grätzel, W. Tress, *Nature Energy* **2018**, 3, 641; d) S. D. Stranks, G. E. Eperon, G. Grancini, C. Menelaou, M. J. Alcocer, T. Leijtens, L. M. Herz, A. Petrozza, H. J. Snaith, *Science* **2013**, 342, 341; e) A. Kojima, K. Teshima, Y. Shirai, T. Miyasaka, *Journal of the American Chemical Society* **2009**, 131, 6050; f) W. S. Yang, B.-W. Park, E. H. Jung, N. J. Jeon, Y. C. Kim, D. U. Lee, S. S. Shin, J. Seo, E. K. Kim, J. H. Noh, *Science* **2017**, 356, 1376.
- [2] a) M. Saliba, T. Matsui, J.-Y. Seo, K. Domanski, J.-P. Correa-Baena, M. K. Nazeeruddin, S. M. Zakeeruddin, W. Tress, A. Abate, A. Hagfeldt, *Energy & Environmental Science* **2016**, 9, 1989; b) N. H. Tiep, Z. Ku, H. J. Fan, *Advanced Energy Materials* **2016**, 6, 1501420; c) S.-H. Turren-Cruz, M. Saliba, M. T. Mayer, H. Juárez-Santiesteban, X. Mathew, L. Nienhaus, W. Tress, M. P. Erodici, M.-J. Sher, M. G. Bawendi, *Energy & Environmental Science* **2018**, 11, 78.
- [3] H.-S. Kim, I.-H. Jang, N. Ahn, M. Choi, A. Guerrero, J. Bisquert, N.-G. Park, *The journal of physical chemistry letters* **2015**, 6, 4633.
- [4] a) N. Aristidou, C. Eames, I. Sanchez-Molina, X. Bu, J. Kosco, M. S. Islam, S. A. Haque, *Nature Communications* **2017**, 8, 15218; b) J. A. Christians, P. Schulz, J. S. Tinkham, T. H. Schloemer, S. P. Harvey, B. J. T. de Villers, A. Sellinger, J. J. Berry, J. M. Luther, *Nature Energy* **2018**, 3, 68; c) Q. Sun, P. Fassel, D. Becker - Koch, A. Bausch, B. Rivkin, S. Bai, P. E. Hopkinson, H. J. Snaith, Y. Vaynzof, *Advanced Energy Materials* **2017**, 7, 1700977.
- [5] a) Y. Chen, Y. Sun, J. Peng, J. Tang, K. Zheng, Z. Liang, *Advanced Materials* **2018**, 30, 1703487; b) M. E. Kamminga, H.-H. Fang, M. R. Filip, F. Giustino, J. Baas, G. R. Blake, M. A. Loi, T. T. Palstra, *Chemistry of Materials* **2016**, 28, 4554; c) R. K. Misra, B.-E. Cohen, L. Iagher, L. Etgar, *ChemSusChem* **2017**, 10, 3712; d) J. Qing, X. K. Liu, M. Li, F. Liu, Z. Yuan, E. Tiukalova, Z. Yan, M. Duchamp, S. Chen, Y. Wang, *Advanced Energy Materials* **2018**, 8, 1800185.
- [6] a) J. Rodríguez-Romero, B. C. Hames, I. Mora-Sero, E. M. Barea, *ACS Energy Letters* **2017**, 2, 1969; b) G. Grancini, C. Roldán-Carmona, I. Zimmermann, E. Mosconi, X. Lee, D. Martineau, S. Narbey, F. Oswald, F. De Angelis, M. Graetzel, *Nature communications* **2017**, 8, 15684; c) J. Yan, W. Qiu, G. Wu, P. Heremans, H. Chen, *Journal of Materials Chemistry A* **2018**, 6, 11063; d) Y. Cho, A. M. Soufiani, J. S. Yun, J. Kim, D. S. Lee, J. Seidel, X. Deng, M. A. Green, S. Huang, A. W. Y. Ho - Baillie, *Advanced Energy Materials* **2018**, 8, 1703392; e) J.-C. Blancon, H. Tsai, W. Nie, C. C. Stoumpos, L. Pedesseau, C. Katan, M. Kepenekian, C. M. M. Soe, K. Appavoo, M. Y. Sfeir, S. Tretiak, P. M. Ajayan, M. G. Kanatzidis, J. Even, J. J. Crochet, A. D. Mohite, *Science* **2017**, 355, 1288; f) T. Zhang, L. Xie, L. Chen, N. Guo, G. Li, Z. Tian, B. Mao, Y. Zhao, *Advanced Functional Materials* **2017**, 27, 1603568; g) T. Zhang, M. I. Dar, G. Li, F. Xu, N. Guo, M. Grätzel, Y. Zhao, *Science Advances* **2017**, 3, 1700841.
- [7] a) F. Yang, G. Kapil, P. Zhang, Z. Hu, M. A. Kamarudin, T. Ma, S. Hayase, *ACS applied materials & interfaces* **2018**, 10, 16482; b) Q. Chen, H. Zhou, Z. Hong, S. Luo, H.-S.

- Duan, H.-H. Wang, Y. Liu, G. Li, Y. Yang, *Journal of the American Chemical Society* **2013**, 136, 622; c) Y. Fu, K. M. Akmal, Z. PuTao, K. Gaurav, M. Tingli, H. Shuzi, *ChemSusChem* **2018**, 11, 2348.
- [8] a) J. Burschka, N. Pellet, S.-J. Moon, R. Humphry-Baker, P. Gao, M. K. Nazeeruddin, M. Grätzel, *Nature* **2013**, 499, 316; b) S. Sun, T. Salim, N. Mathews, M. Duchamp, C. Boothroyd, G. Xing, T. C. Sum, Y. M. Lam, *Energy & Environmental Science* **2014**, 7, 399.
- [9] L. Jianfeng, J. Liangcong, L. Wei, L. Feng, P. N. K., S. A. D., T. Cheng - Min, B. Udo, S. A. N., C. Yi - Bing, S. Leone, *Advanced Energy Materials* **2017**, 7, 1700444.
- [10] C. Chen, Y. Xu, S. Wu, S. Zhang, Z. Yang, W. Zhang, H. Zhu, Z. Xiong, W. Chen, W. Chen, *Journal of Materials Chemistry A* **2018**, 6, 7903.
- [11] T. P. Gujar, T. Unger, A. Schönleber, M. Fried, F. Panzer, S. van Smaalen, A. Köhler, M. Thelakkat, *Physical Chemistry Chemical Physics* **2018**, 20, 605.
- [12] X. Zheng, B. Chen, J. Dai, Y. Fang, Y. Bai, Y. Lin, H. Wei, X. C. Zeng, J. Huang, *Nature Energy* **2017**, 2, 17102.
- [13] Y.-K. Ren, X.-H. Ding, Y.-H. Wu, J. Zhu, T. Hayat, A. Alsaedi, Y.-F. Xu, Z.-Q. Li, S.-F. Yang, S.-Y. Dai, *Journal of Materials Chemistry A* **2017**, 5, 20327.
- [14] a) B. E. Cohen, M. Wierzbowska, L. Etgar, *Advanced Functional Materials* **2017**, 27, 1604733; b) D. H. Cao, C. C. Stoumpos, O. K. Farha, J. T. Hupp, M. G. Kanatzidis, *Journal of the American Chemical Society* **2015**, 137, 7843; c) R. L. Milot, R. J. Sutton, G. E. Eperon, A. A. Haghighirad, J. Martinez Hardigree, L. Miranda, H. J. Snaith, M. B. Johnston, L. M. Herz, *Nano letters* **2016**, 16, 7001.
- [15] F. Yang, G. Kapil, P. Zhang, Z. Hu, M. A. Kamarudin, T. Ma, S. Hayase, *ACS Applied Materials & Interfaces* **2018**, 10, 16482.

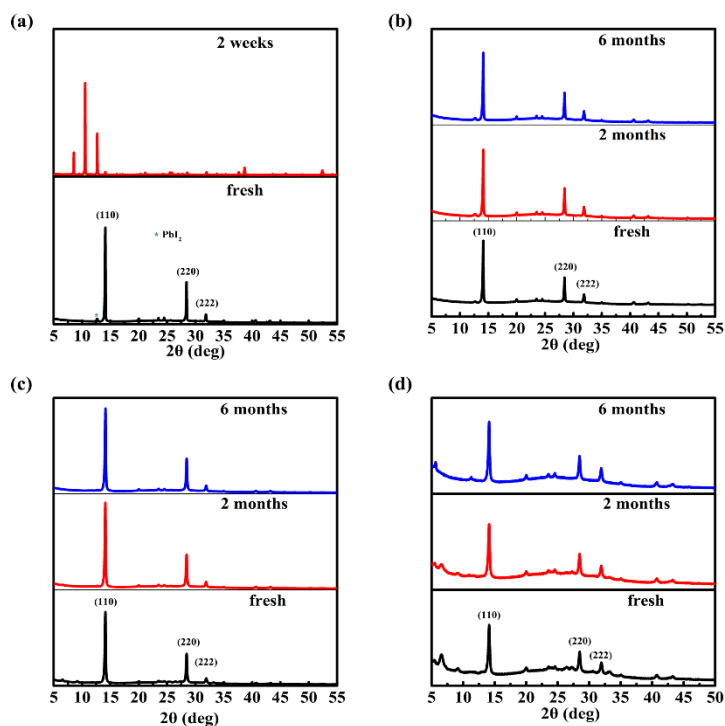


Figure 1. X-ray diffraction of 2D/3D-X (X: 0, 0.02, 0.05, 0.10) perovskite film on glass substrate. The samples was stored in ~60% RH humidity at ambient atmosphere in the dark condition without encapsulation. (a) 2D/3D-0 (b) 2D/3D-0.02 (c) 2D/3D-0.05 (d) 2D/3D-0.10.

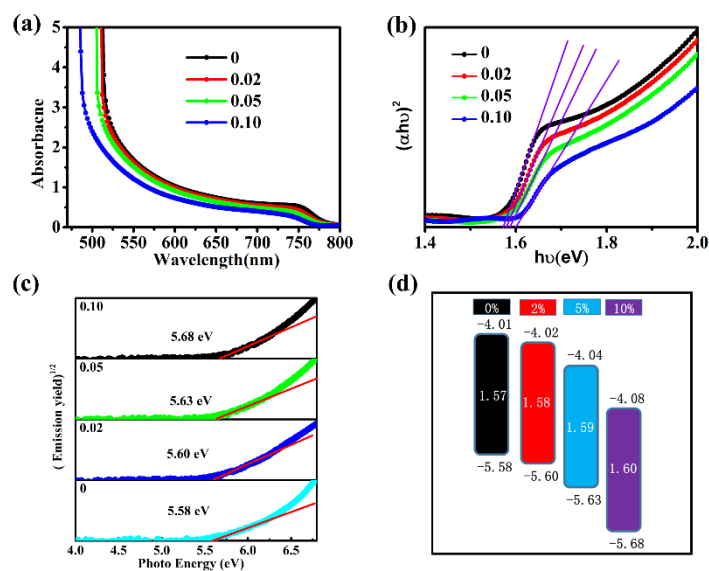


Figure 2. (a) The UV-vis absorption spectra for 2D/3D-X (b) $(\alpha h\nu)^2$ versus energy for 2D/3D-X (x, 0, 0.02, 0.05, 0.10) perovskite films on FTO glass substrates. (c) The PESA for the for 2D/3D-X (x, 0, 0.02, 0.05, 0.10) perovskite films on FTO glass substrates. (d) Corresponding electronic structure diagrams of for 2D/3D-X (x, 0, 0.02, 0.05, 0.10) perovskite.

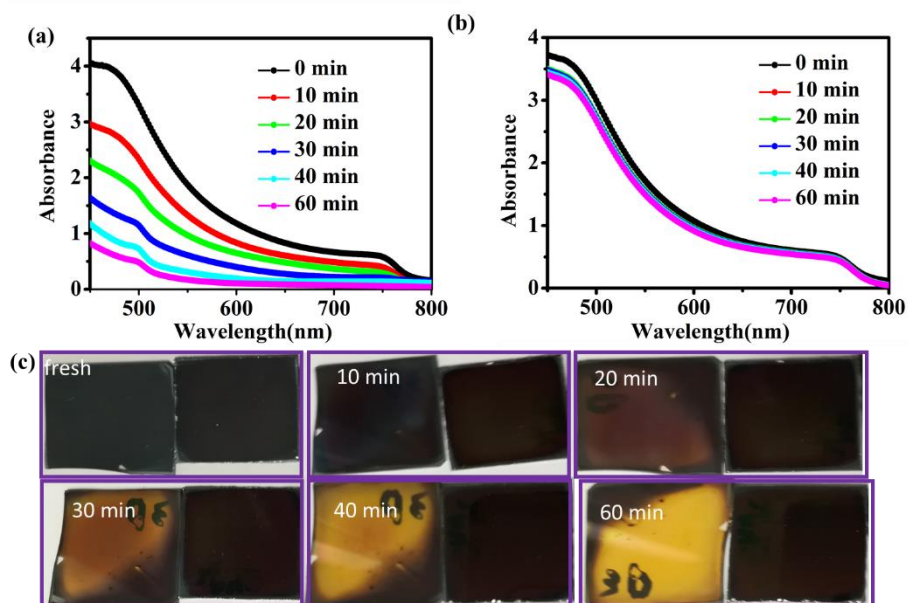


Figure 3. The UV-vis spectra of 2D/3D-0, (b) 2D/3D-0.02, (c) Color change of perovskite film after UV Ozone treatment. Left: 2D/3D-0, Right 2D/3D-0.02.

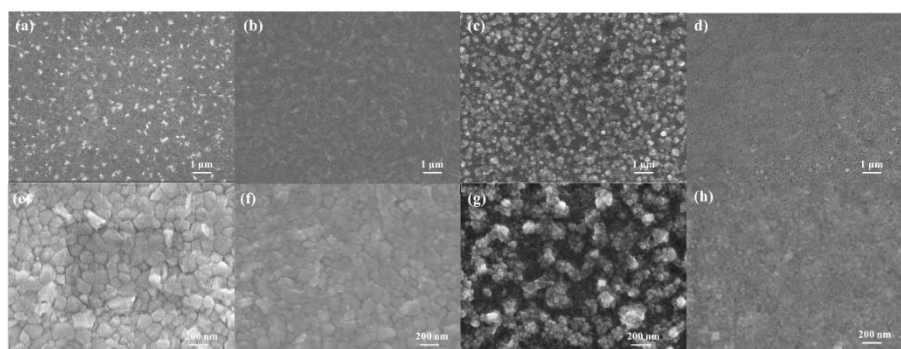


Figure 4. 2D/3D-X perovskite film on FTO substrates. (a)(e) 2D/3D-0; (b) (f) 2D/3D-0.02; (c) (g) 2D/3D-0.05; (d) (h) 2D/3D-0.10.

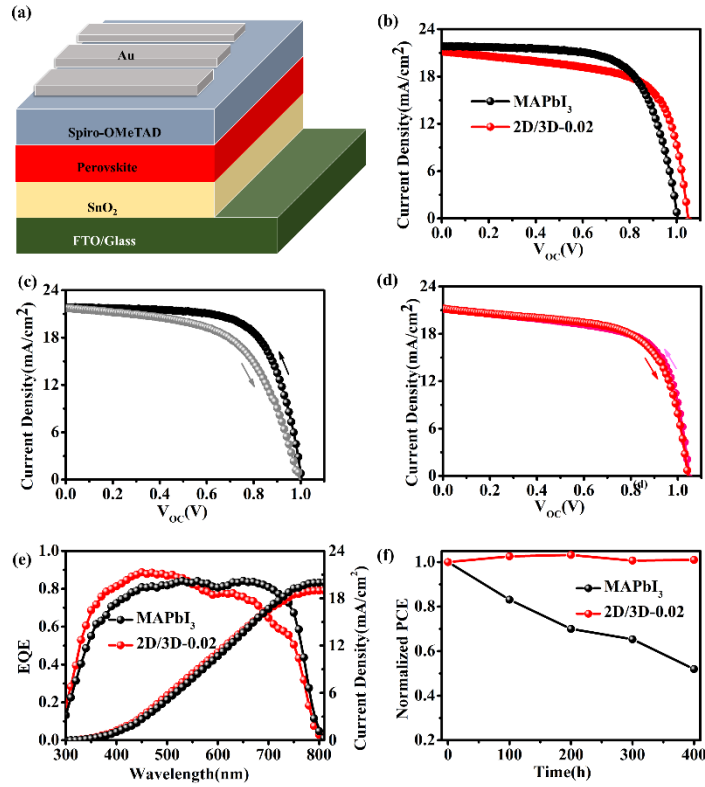


Figure 5. (a) Schematic structure of FTO/SnO₂/perovskite/Spiro-OMeTAD/Au planar perovskite solar cells. (b) J-V curves in reverse direction of 2D/3D-0 and 2D/3D-0.02 planar perovskite solar cells. (c) J-V curves of the champion 2D/3D-0 perovskite solar cell under reverse and forward voltage scans. (d) J-V curves of the champion 2D/3D-0.02 perovskite solar cell under reverse and forward voltage scans. (e) EQE spectra of 2D/3D-0 and 2D/3D-0.02 planar perovskite solar cells. (f) Stability test for 400 h of the champion device under ambient atmosphere without sealing in dark condition under average humidity of around 60%.

$$HI = \frac{J_R(0.8V_{OC}) - J_F(0.8V_{OC})}{J_R(0.8V_{OC})} \quad \text{Equation 1}$$

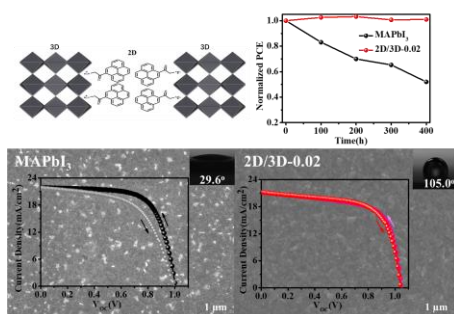
$J_R(0.8V_{OC})$ and $J_F(0.8V_{OC})$ represent photocurrent values at 0.8 of the V_{OC} value for the reverse and forward scan direction.

A novel organic compound 1-(ammonium acetyl) pyrene has successfully introduced for preparing the 2D/3D hetero structured MAPbI₃ perovskite. Because of the functional organic pyrene group with high humidity resistance and strong absorption in the ultraviolet region, the 2D/3D perovskite film showed notable stability in humid air atmosphere and ultraviolet irradiation. The power conversation efficiency of 2D/3D perovskite solar cells is comparable with MAPbI₃ with nearly no hysteresis.

Keyword Two-dimensional; MAPbI₃; Planar solar cells; Stability; UV light stability.

*Fu Yang**, *Putao Zhang*, *Muhammad Akmal Kamarudin*, *Gaurav Kapil*, *Tingli Ma*, *Shuzi Hayase**

Addition Effect of Pyreneammonium Iodide to Methylammonium Lead Halide Perovskite-2D/3D Hetero Structured Perovskite with Enhanced Stability



Addition Effect of Pyreneammonium Iodide to Methylammonium Lead Halide Perovskite-2D/3D Hetero Structured Perovskite with Enhanced Stability

*Fu Yang, Putao, Zhang, Muhammad Akmal Kamarudin, Gaurav Kapil, Tingli Ma, Shuzi Hayase**

Kyushu Institute of Technology, 204 Hibikino Wakamatsu-ku, Kitakyushu 808-0196, Japan

Corresponding Author

yang-fu@edu.life.kyutech.ac.jp; hayase@life.kyutech.ac.jp

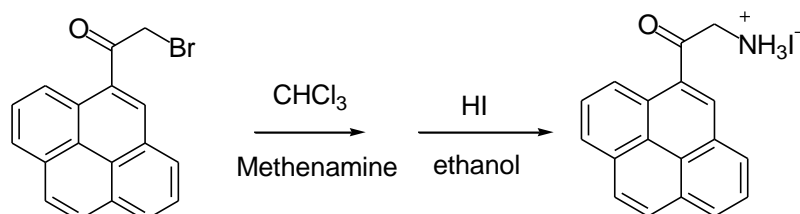
Experimental section

Figure S1 Synthetic route of PYEHI

Synthesis of PYEHI

Figure S1 shows the synthetic route of PYEHI. 4.0 g 1-(Bromoacetyl)pyrene (Aldrich, 97%), 1.9 g hexamethylenetetramine (Aldrich, 99%) were added into 60 ml chloroform (Aldrich, 99%) in a round-bottom flask. The solution was stirred at room temperature for 12h. The precipitate

was filtered and washed with chloroform 3 times to get the slight white solid. The solid was directly added into 100 ml ethanol (TCI, 99.5%). Then 6 ml hydriodic acid (Aldrich, 57 wt. % in water) was slowly added into the solution. The solution was stirred at 45 °C for 4 h and then cooled at room temperature. The precipitate was filtered. After washing with ethanol, acetone, and diethyl ether, compound PYEHI was obtained as a slight white solid. ESI-MS (m/z): calcd. $[M^+]$ for $[C_{18}H_{14}NO]^+$ 260.11, found 260.11. Elemental analysis: calcd, C, 55.83, H, 3.64, N, 3.62. Found, C 56.87, H, 3.81, N, 3.66.

Preparation of perovskite solar cells

Fluorine-doped tin oxide (FTO glass, Nippon Sheet Glass Co. Ltd) substrates were etched with r hydrochloric acid solution and zinc powder. Tin (II) chloride (Aldrich, 98 %) was dissolved in ethanol (Wako, 99.8 %) to form 0.1 M $SnCl_2$ solution. Then the $SnCl_2$ solution was spin-coated on the cleaned FTO glass at 2000 rpm for 30 seconds. The substrate was annealed at 180 °C for 60 min utes on a hot plate to form a dense SnO_2 electron transport layer. The perovskite solution was prepared by dissolving 239 mg MAI (TCI, 98 %) and 692 mg PbI_2 (TCI, 99.99 %) into 0.2 mL dimethyl sulfoxide (DMSO, Aldrich, 99.8 %) and 0.8 mL dimethylformamide (DMF, Aldrich, 99.8 %) to achieve 1.5 M $MAPbI_3$ perovskite precursor solution. For preparing the 2D/3D perovskite precursor solution, keeping the PbI_2 at 1.5M and adding a proper PYEHI and MAI into 0.2 mL dimethyl sulfoxide (DMSO, Aldrich, 99.8 %) and 0.8 mL dimethylformamide. The Spiro-MeOTAD solution was prepared by mixing 72.3 mg Spiro-MeOTAD (Aldrich, 99 %), 28.8 μ L tert-butylpyridine (Aldrich, 96 %) , 17.5 μ L Li-TFSI (Aldrich, 99.95 %) (520 mg/mL in acetonitrile) and 29 μ L FK209 (Aldrich, 99 %) (300 mg/mL in acetonitrile) in 1 mL chlorobenzene solution. The perovskite layer was prepared on the mesoporous TiO_2 substrate by adding 0.1 mL perovskite precursor solution and spin-coated at 4000 rpm for 25 s. 0.5 mL ethyl acetate (99.8 %, Aldrich) antisolvent was dripped during the spin-coated progress.^[15] The spin-coated perovskite film was annealed at 100 °C for 10 min. The Spiro -MeOTAD layer spin-coated on the perovskite layer at 4000 rpm for 30 s. Finally, Au electrode with 80 nm thickness was deposited on the Spiro film by thermal evaporation.

Characterization

Solar cell performance was measured by a solar simulator (CEP-2000SRR, Bunkoukeiki Inc., AM 1.5G 100 $mWcm^{-2}$) and a mask with exposure area 0.10 cm^2 was used during the photovoltaic measurements with a 0.1 V/s scanning rate in reverse (from the open-circuit voltage (V_{oc}) to the short-current density (J_{sc})) and forward (from J_{sc} to V_{oc}) modes under standard global AM 1.5 illumination. The IPCE spectra were recorded using a monochromatic Xenon lamp (Bunkouki CEP-2000SRR). X-ray Diffraction (XRD) Study. The surface morphology of the samples was observed through a scanning electron microscope (SEM) (JEOL, Neoscope, JCM-6000) and a Bruker Innova atomic force microscopy (AFM) (JSPM-5200). The XRD patterns were obtained by a Rigaku Smartlab X-ray diffractometer with monochromatic $Cu-K\beta$ irradiation (45 kV/200 mA). The UV-Vis measurement was performed using a JASCO V-670. Spectrophotometer. Photoelectron yield spectroscopy (PYS) was used to determine the valence band using a Bunkoukeiki KV205-HK ionization energy measurement system with – 5.0 V of applied voltage under 10^{-4} Pa vacuum.

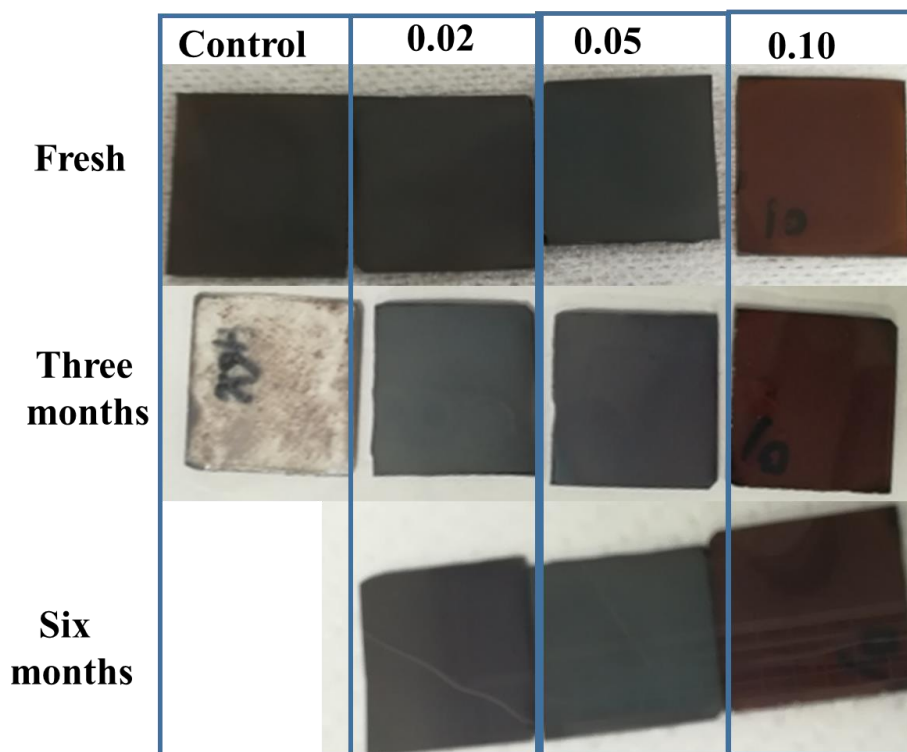


Figure S1 The perovskite films after kept at ambient atmosphere at different time.

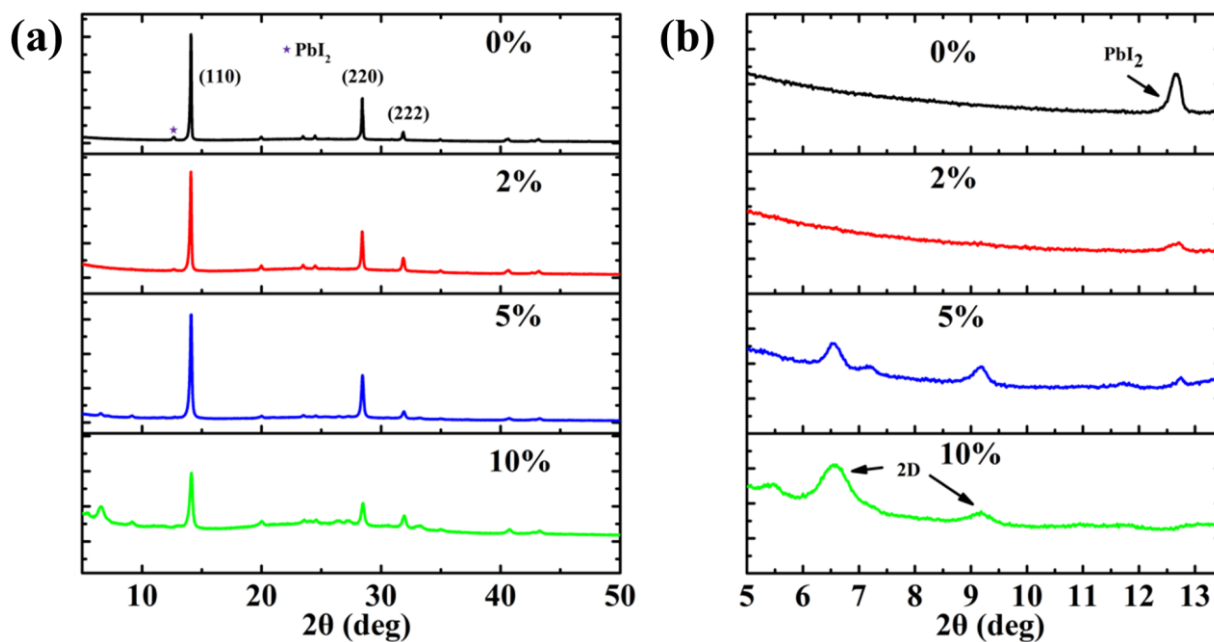


Figure S2 X-ray diffraction of $(\text{PEY}_2\text{PbI}_4)_x\text{MAPbI}_3$ (0, 0.02, 0.05, 0.10) perovskite film on glass substrate. (c) The zoomed XRD spectra.

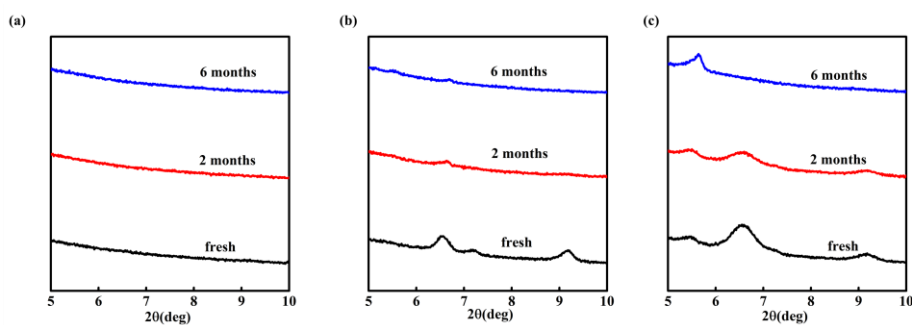


Figure S3 X-ray diffraction of $(\text{PEY}_2\text{PbI}_4)_x\text{MAPbI}_3$ (0.02, 0.05, 0.10) perovskite film. The samples was stored in $\sim 60\%$ RH humidity at ambient atmosphere in the dark condition without encapsulation. (a) $x=0.02$, (b) $x=0.05$, (c) $x=0.10$.

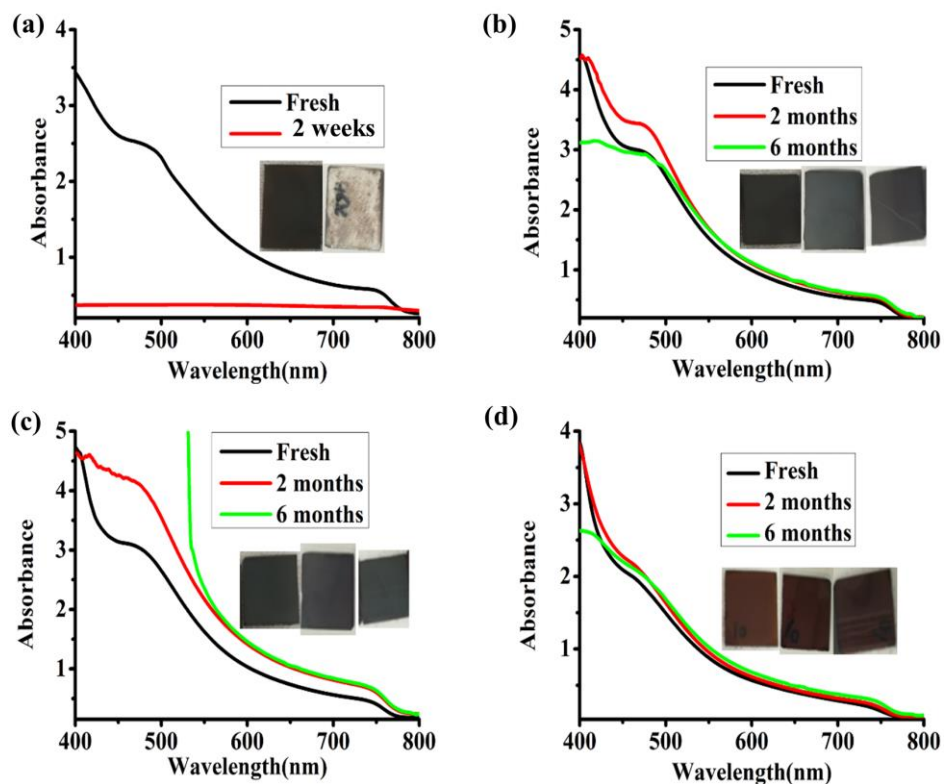


Figure S4 UV-vis spectra of 2D/3D-X (X: 0, 0.02, 0.05, 0.10) perovskite film on glass substrate. The samples was stored in $\sim 60\%$ RH humidity at ambient atmosphere in the dark condition without encapsulation. (a) 2D/3D-0 (b) 2D/3D-0.02 (c) 2D/3D-0.05 (d) 2D/3D-0.10.

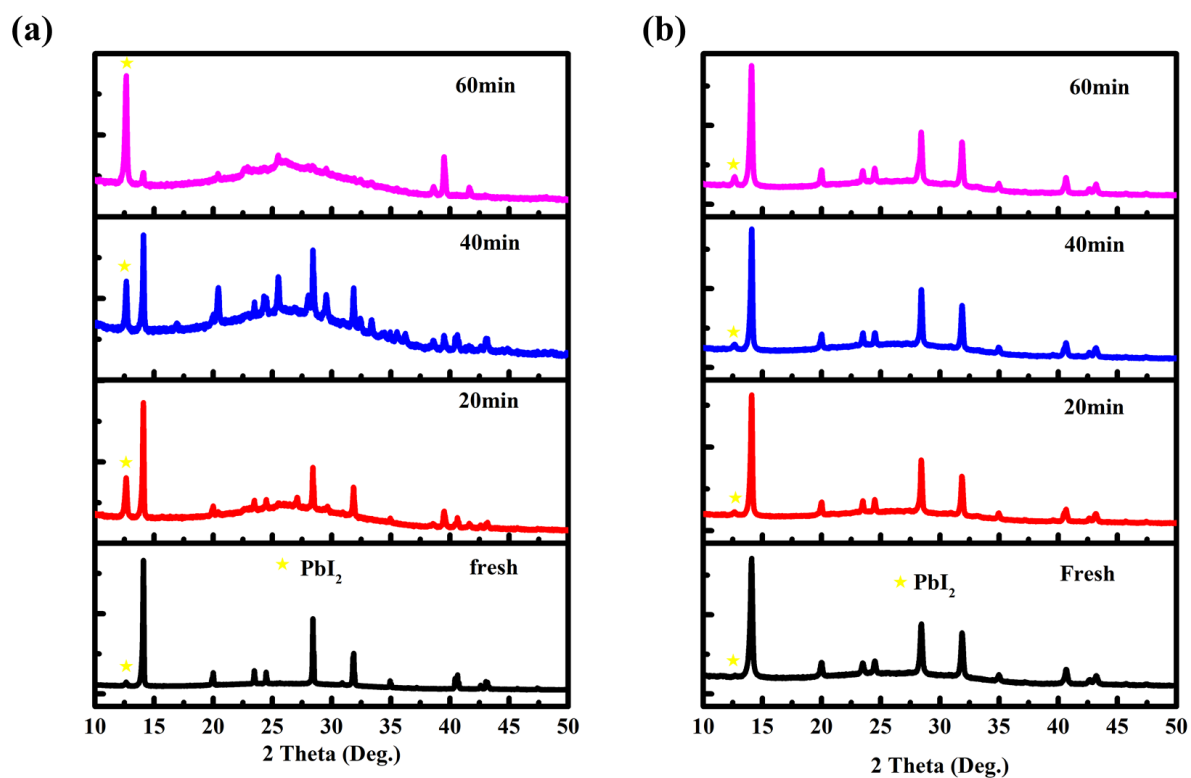


Figure S5 X-ray diffraction of (a) 2D/3D-0 and (b) 2D/3D-0.02 perovskite film under UV Ozone treatment for different time.

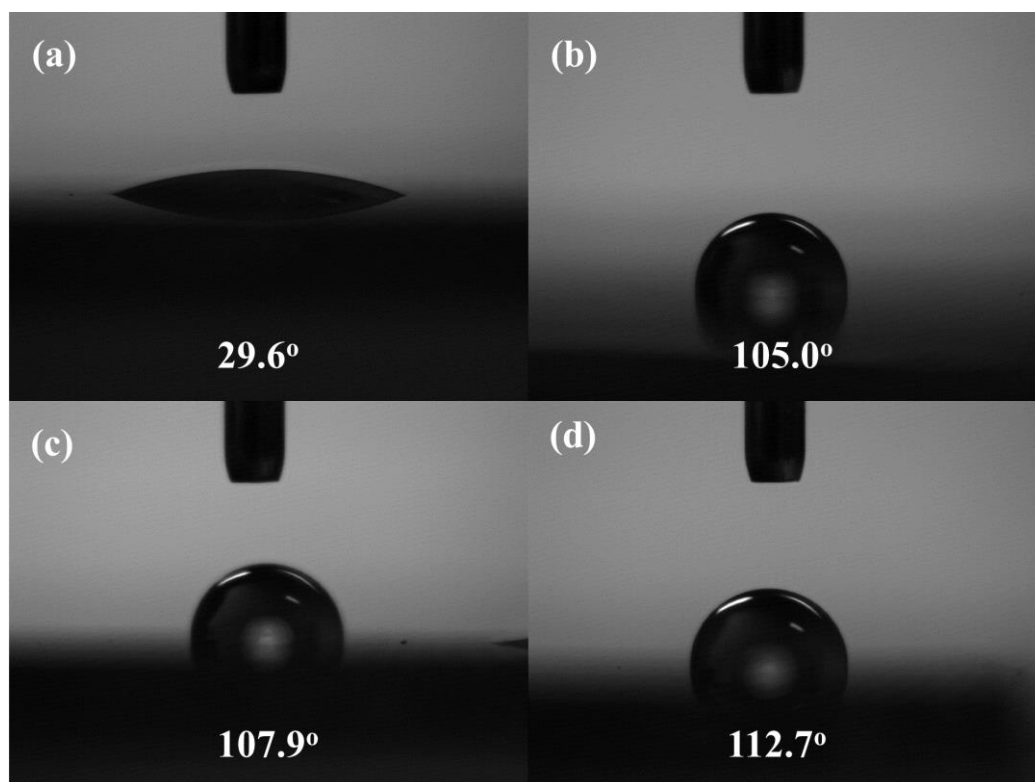


Figure S6 Contact-angle test for the $(\text{PEY}_2\text{PbI}_4)_x\text{MAPbI}_3$ (0, 0.02, 0.05, 0.10) perovskite film with water droplets. (a) MAPbI_3 ; (b) $(\text{PEY}_2\text{PbI}_4)_{0.02}\text{MAPbI}_3$; (c) $(\text{PEY}_2\text{PbI}_4)_{0.05}\text{MAPbI}_3$; (d) $(\text{PEY}_2\text{PbI}_4)_{0.10}\text{MAPbI}_3$.

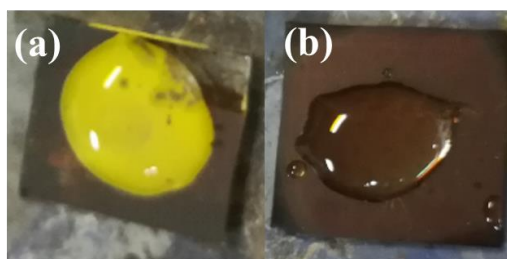


Figure S7 One drop water on MAPbI_3 (a) and $(\text{PEY}_2\text{PbI}_4)_{0.02}\text{MAPbI}_3$ (b) perovskite film.

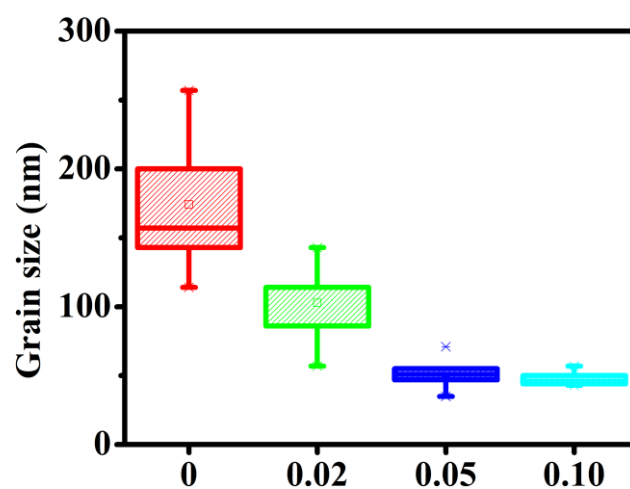


Figure S8 The statistical distribution of the particle size for $(\text{PEY}_2\text{PbI}_4)_x\text{MAPbI}_3$ (0, 0.02, 0.05, 0.10) perovskite film.

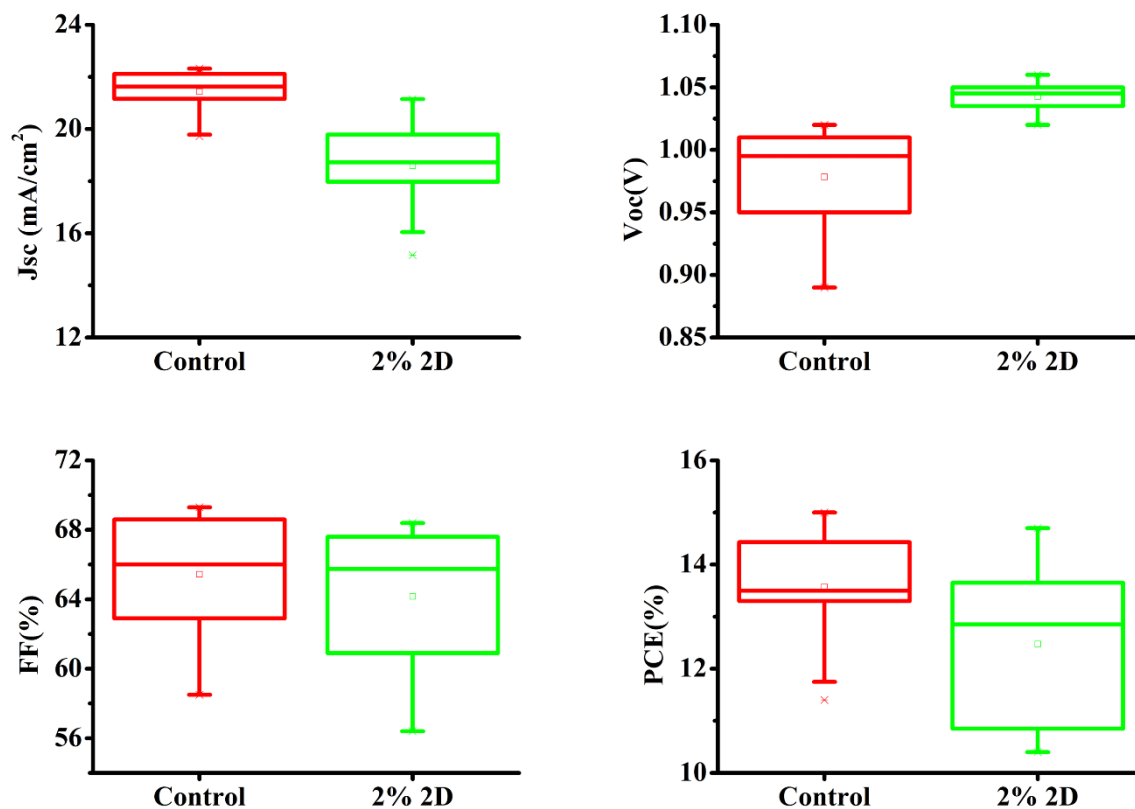


Figure S9 Photovoltaic statistics for the planar perovskite solar cells based on **MAPbI₃** and **(PEY₂PbI₄)_{0.02}MAPbI₃** materials. (a) J_{sc} , (b) V_{oc} , (c) Fill factor, (d) Efficiency. The boxes represent 40 data from the V_{oc} -to- J_{sc} scan direction.